

Resonance-Fluorescence Studies. I. ^{45}Sc , ^{69}Ga , and ^{71}Ga [†]

Raymond G. Arnold,* Edward C. Booth, and William J. Alston, III[‡]

Boston University, Boston, Massachusetts 02215

(Received 31 January 1972)

Resonant scattering of bremsstrahlung was used to measure $g\overline{W}\Gamma_0\Gamma_0/\Gamma$ for 13 transitions in ^{45}Sc and 18 transitions in $^{69,71}\text{Ga}$ below 2.5 MeV. New level widths were measured by direct comparison of resonant scattering from levels of known width. Where branching ratios are known, radiative widths to the ground state Γ_0 are deduced. Comparisons are made between level widths measured in this work and in other measurements. The transition strengths in ^{69}Ga are compared with the most recent nuclear model.

I. INTRODUCTION

Experimental work in ^{45}Sc (Refs. 1–6), ^{69}Ga (Refs. 7–11), and ^{71}Ga (Refs. 7, 11, and 12) has established the level schemes up to about 2.0 MeV. $B(E2)$ measurements on three transitions¹³ and one level width measurement¹ have been made in ^{45}Sc , and three widths are known in ^{69}Ga (Ref. 14). The present work reports transition strengths in all three nuclei.

Transition probabilities are not calculated in the theoretical studies of ^{45}Sc (Refs. 15–17), but Johnstone¹⁷ predicted a series of levels comparable to the experimentally known sequence with spins $\frac{3}{2}^+$, $\frac{5}{2}^+$, and $\frac{7}{2}^+$ using a rotational $k=\frac{3}{2}$ band built on a $d_{3/2}$ hole state in ^{46}Ti . Scholz and Malik,¹⁸ using a Coriolis-plus-pairing-force model, explained the general features of nuclei near gallium, but their calculations for ^{71}Ga were based on incorrect experimental data. The intermediate-coupling model by Paradellis and Hontzeas¹⁹ reproduced the level scheme of ^{69}Ga fairly well up to about 1.5 MeV, and predicted theoretical transformation probabilities. In order to provide experimental transition strengths for comparison with model predictions and to motivate future calculations, ground-state transition strengths in ^{45}Sc , ^{69}Ga , and ^{71}Ga from 400 to 2500 keV were measured by means of bremsstrahlung resonance fluorescence. Partial widths were found for 13 transitions in ^{45}Sc and 18 transitions in $^{69,71}\text{Ga}$.

II. FLUX DETERMINATION

The primary difficulty with measuring transition strengths in resonant-scattering experiments is the problem of determining the incident photon flux. The number of resonantly scattered photons is proportional to $\int N(E_R)\sigma(E_R)dE$, where $\sigma(E_R)$ is the absorption cross section and $N(E_R)$ is the number of incident photons per energy interval near the resonant energy E_R . A number of investigators^{20–23}

using bremsstrahlung resonance fluorescence have determined $N(E_R)$ in separate runs by measuring the yield from comparison scatterers containing nuclei with excited levels of known width, branching, and multipole mixing. We determined new widths by *simultaneously* scattering bremsstrahlung from scatterers containing nuclei with known and unknown widths. New transition strengths were obtained by direct comparison of yields of resonantly scattered radiation. This comparison eliminates many errors due to fluctuations in accelerator conditions and geometry.

Since the accuracy of this comparison method depends upon the knowledge of widths used for calibration, a literature search²⁴ was conducted and measurements performed upon many previously measured transitions. Figure 1 shows the relative flux through the scatterer at photon energies 10% below the electron energy E_T derived from those measurements. The flux points are described as relative because no attempt was made to determine accurately the absolute detector efficiency (see Appendix I). The literature value for a calibration width is defined to be the weighted average of selected measurements (see Appendix II). The curve in Fig. 1 represents the average of over 100 width measurements reported in the literature.

Each calibration level was investigated at two or more electron energies and the scattering yields were fitted with the excitation function shape²⁵ to determine the yield at $0.9E_T$. The relative flux was derived from the yield at $0.9E_T$ using the average literature value for the width in Eq. (1) of the Appendix I. Each flux point in Fig. 1 represents the average of several such excitation functions on each state. The smaller error bars indicate the statistical error in the scattering yield and the larger indicate the geometric sum of that statistical error and the uncertainty in the literature value for the calibration width.

The flux points in Fig. 1 were fitted with a quad-

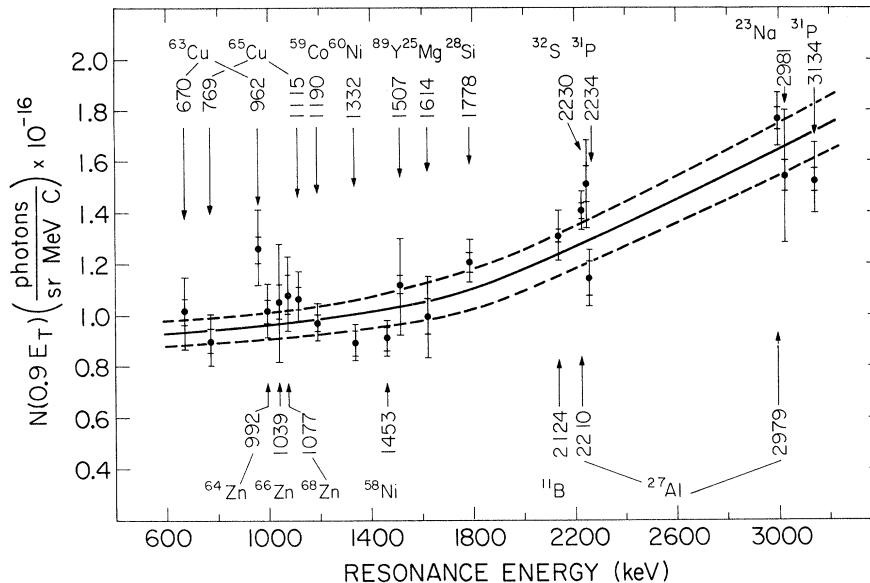


FIG. 1. The flux curve. Plotted is the photon flux on the target at $E_R = 0.9T$ determined from excitation functions on levels of known width and branching. The error bars are discussed in the text. The solid curve represents a weighted least-squares fit and the dashed lines represent the estimated over-all uncertainty in the flux.

ratio function of energy represented by the solid line, by means of a weighted least-squares procedure with the normalized $\chi^2 = 1.696$. A straight-line fit yielded a $\chi^2 = 1.981$. The assigned error of 6% in the flux, represented by the dashed lines in Fig. 1, is 1 standard deviation of the fitted function multiplied by 1.7 to account for the uncertainty introduced by the relatively large deviations of some points from the fit.

The measurements represented in Fig. 1 were taken with a standard procedure using uniform-shaped scatterers in the same experimental arrangement, and the individual points reproduced several times. We are confident that the large scatter among the flux points primarily represents uncertainty in the knowledge of the transition widths and not our experimental errors.

Due to beam-handling difficulties at low electron energies, the flux curve of Fig. 1 was not used for levels under 600 keV. The 543-keV level in ^{45}Sc , the 574-keV level in ^{69}Ga , and the 389- and 487-keV limits in ^{71}Ga were measured relative to the 477-keV level of ^7Li using the width $\Gamma_0 = 6.16 \pm 0.46$ meV.²⁶

III. GEOMETRY AND EXPERIMENTAL PROCEDURE

The scattering geometry employed is depicted in Fig. 2. The electron beam from the 4-MeV Van de

Graaff in the High Voltage Research Laboratory at Massachusetts Institute of Technology was deflected 90° from the vertical, passed through a 54.5-mg/cm² platinum foil, and stopped in a 0.63-cm water-cooled aluminum stopper. The 35-cm³ coaxial Ge(Li) detector was located at an angle of 125° from the incident beam in order to minimize the corrections for angular-correlation effects. The scatterers were each 500 to 1000 g of powdered metals, or oxides, or some multiple compounds, all of known purity, sealed in light rectangular cardboard containers 10 by 20 cm. The aluminum, copper, and magnesium scatterers were solid metal. The scandium scatterer was 500 g of Sc_2O_3 and the gallium was 512 g of small ingots. Multiple scatterers were placed one behind the other as shown in Fig. 2. Correction was made to the yields from the aluminum scatterer for resonance absorption in the aluminum beam stop.

Lead filters between the detector and the scatterer preferentially absorbed low-energy Compton-scattered photons, reducing the total counting rate and keeping the pulse pileup losses in a pulser peak below 8%. At total counting rates $< 2 \times 10^4$ sec⁻¹ with RC pulse shaping of 800 nsec, the peak widths (full width at half maximum) were 3.3 keV at 1.0 MeV and 7.0 keV at 3.0 MeV. Large peak widths and analyzer nonlinearity at variable counting rates produced energy errors of at least 1 keV.

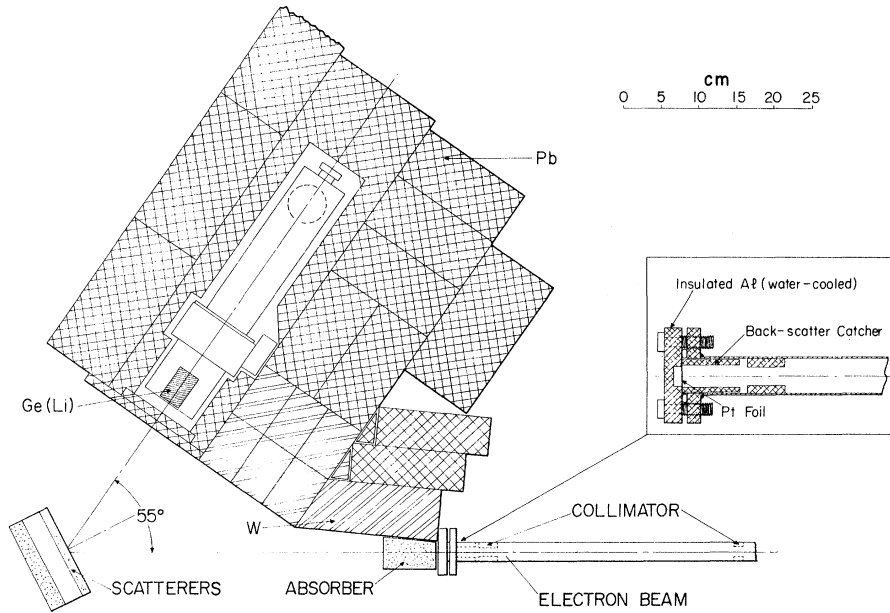


FIG. 2. Bremsstrahlung resonance-fluorescence scattering geometry.

IV. DATA ANALYSIS

A. Analysis of Spectral Data

The program called SAMPO²⁷ with routines for plotting, specifying energy and peak shape calibrations, searching for peaks, and finding peak areas, was used to analyze the data (illustrated in Fig. 3). The program was modified in the present work²⁴ to include a gain shifting routine for summing spectra from separate runs. With the SAMPO program it was possible to extract areas of peaks that were nearly unresolved. The peak shapes were deter-

mined from fits to strong isolated peaks. A deterioration of the quality of the fits using fixed-shape parameters indicated the presence of unresolved γ rays. Figure 4 shows the analysis of a doublet at 1106-1109 keV in ^{69,71}Ga. Energy assignments were made using radioactive sources and γ rays from the calibration scatterers.

B. Analysis of Yields

The yield of resonantly scattered photons was derived from the peak counts by making solid-angle, absorption, and detector-efficiency correc-

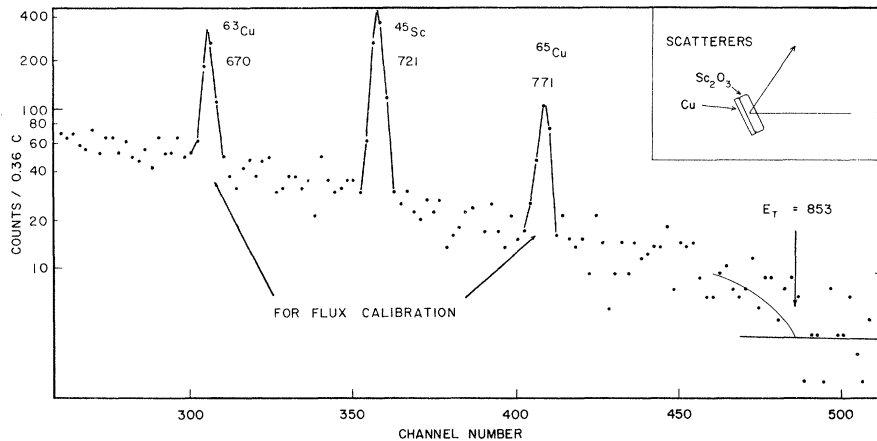


FIG. 3. Pulse-height distribution for resonant scattering from scandium and copper. The energies are in keV. E_T is the bremsstrahlung end-point energy.

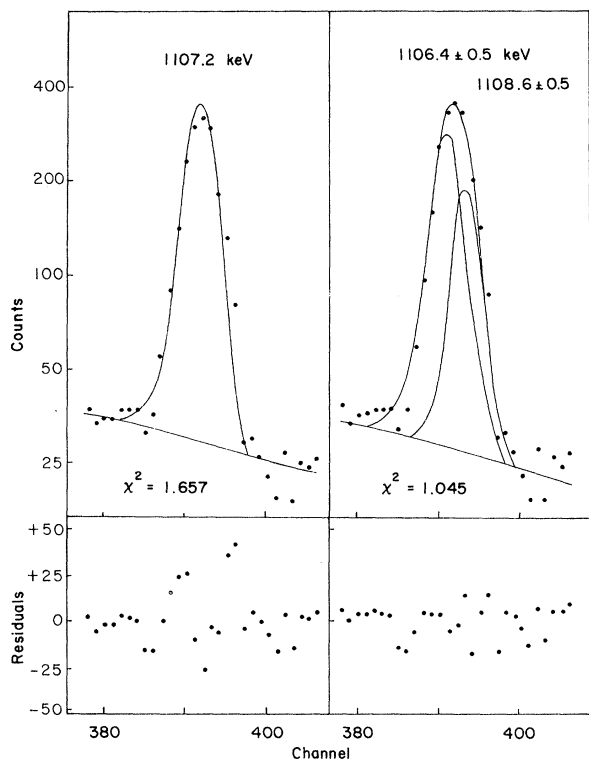


FIG. 4. SAMPO fits to the gallium doublet at 1106–1109 keV. On the left the data are fitted with a single peak with a fixed-shape parameter determined previously from fits to strong isolated peaks. The oscillation in the residuals and the large χ^2 value indicate that the peak is a doublet. On the right is an improved fit including two peaks.

tions for the scatterer geometry (see Appendix I).

Excitation functions of the resonance-fluorescence yield [Eq. (1), Appendix I] were obtained for levels of known and unknown width simultaneously, and these were fitted to the known excitation functions shape.²⁵ $N(E_R)$ was found using the literature values for the known widths adjusted to fit the solid line in Fig. 1, and the unknown level widths were found using Eq. (1), Appendix I. The new width derived was used in an iterative procedure to correct for resonant absorption in the scatterer. The error for each new width is the geometric sum of the statistical error and the uncertainty in $N(E_R)$.

C. Background and Limits on Widths

Spectra were added in order to improve the counting statistics for weak transitions. In the

absence of detectable γ rays the upper limit on peak area was set at 3 standard deviations above background. This criterion was found to be conservative by testing the peak-searching program using small peaks of known area superimposed upon various backgrounds.

A series of runs with no scatterer was taken to find possible accelerator-produced background. With the exception of the ^{28}Si transition at 1778 keV, there were no detectable γ rays from resonance fluorescence in the laboratory materials or from neutrons produced above 2.23 MeV by the (γ, n) reaction in deuterium present in the cooling water.

V. RESULTS AND DISCUSSION FOR ^{45}Sc , ^{69}Ga , AND ^{71}Ga

A. General

A systematic search for resonance fluorescence from known levels was made up to 2.5 MeV in ^{45}Sc and up to 2.0 MeV in gallium, where theoretical and experimental information about the level schemes is sparse.

Except for a few of the very weak transitions, each peak was present in the spectra at two or more electron energies. The results listed in column 5 in Tables I, III, and IV are the weighted average of the scattering widths $g\bar{W}\Gamma_0\Gamma_1/\Gamma$ derived from the individual runs. Also listed are the partial width limits for levels showing no resonance fluorescence in this work. The partial widths to the ground state Γ_0 in the sixth column were deduced using the branching ratios in column 4 and the value $\bar{W}(125^\circ) = 1.0$. The uncertainty in Γ_0 includes the error in the branching ratio but not the uncertainty in the approximation $\bar{W}(125^\circ) = 1.0$. For Sc and Ga, $0.95 \leq \bar{W}(125^\circ) \leq 1.0$ except when $\delta^2 > 2$ for the $\frac{7}{2}^- \rightarrow \frac{3}{2}^- \rightarrow \frac{7}{2}^-$ transitions in Sc and the $\frac{3}{2}^- \rightarrow \frac{5}{2}^- \rightarrow \frac{3}{2}^-$ transitions in Ga.

B. ^{45}Sc Results

The results²⁸ of measurements in ^{45}Sc are presented in Table I. In column 2 are the spins and parities from the literature, except in the case of the 1237- and 2431-keV levels where it is possible to exclude certain spin possibilities by combining our results with previous work. The 543- and 974-keV levels decay to both the first excited state and the ground state, and the Γ_0 is deduced from the yields of the two deexcitation modes. In Table II are the mixing ratios and $M1$ strengths deduced from the comparison of the present measurements with the weighted average of selected $E2$ widths from the literature.

TABLE I. ^{45}Sc levels and results.

Level energy ^a (keV)	$J\pi$ ^a	E_γ This work (keV)	Γ_0/Γ or Γ_1/Γ	$g\overline{W}\Gamma_0\Gamma_0/\Gamma$ This work (meV)	Γ_0 Deduced (meV)
g.s.	$\frac{7}{2}^-$...			
12.4(2)	$\frac{3}{2}^+$...	1.0 ^b	c	...
376.7(6) ^d	$\frac{3}{2}^-$...	0.92 ^d	c	...
543.1(6) ^d	$\frac{5}{2}^+$	531(2) ^e 543(2)	0.58(1) ^{d, e} 0.42(1) ^d	0.019(4) ^e 0.011(3)	... 0.039(8)
720.5(5) ^d	$\frac{5}{2}^-$	720(1)	1.0 ^b	1.58(16)	2.11(21)
939.1(9) ^d	$\frac{1}{2}^+$...	0.0
974.3(7) ^d	$\frac{7}{2}^{+d}$	962(2) ^e 974(2)	0.32(1) ^{d, e} 0.58(1) ^d	0.062(9) ^e 0.08(1)	... 0.17(3)
1068.4(10) ^d	$\frac{3}{2}^-$...	0.0 ^d
1237.4(9) ^d	$(\frac{11}{2})^-$ ^f	1237(2)	1.0 ^d	0.38(2)	0.58(3)
1409.0(10) ^d	$(\frac{9}{2})^-$ ^d	1409(1)	0.91(4) ^d	1.36(11)	1.87(16)
1433.5(10) ^d	$(\frac{9}{2})^{+d}$...	0.10(2) ^d	<0.2	...
1474(3)	<0.2	...
1557(3)	$(\frac{1}{2}, \frac{3}{2})^-$...	0.0 ^b	<0.2	...
1661.8(7) ^d	$(\frac{5}{2}-\frac{3}{2})^-$ ^d	1663(2)	0.83(4) ^d	3.2(3)	3.9(4) g^{-1}
1799(5)	...	1798(2)	0.23(3) ^g	0.22(5)	0.94(21) g^{-1}
1897(5)	1.0 ^g	<1.0	...
1936(5)	c	...
2031.0(10) ^d	$(\frac{11}{2})^{+d}$	<0.5	...
2095(5)	...	2093(2)	0.78(12) ^g	47(2)	60(9) g^{-1}
2106(5)	<0.5	...
2223(5)	<0.5	...
2291(5)	...	2291(3)	...	1.28(8)	...
2303(5)	0.0 ^g	<0.5	...
2341(5)	$(\frac{3}{2})^-$ ^f	2341(2)	...	16(1)	...
2351(5)	0.02 ^{b, h}	<0.5	...
2531(5)	0.0	<2	...
2562(5)	<2	...
2590(5)	...	2592(2)	0.64(9) ^g	8.9(5)	14(2) g^{-1}

^a Except where noted Ref. 1.^b Reference 1.^c No data taken for these levels.^d Reference 2.^e Branch to the first excited state. Transition strength in column 5 is $g\overline{W}\Gamma_0\Gamma_0/\Gamma$.^f See discussion in the text.^g Private communication from J. C. Manthuruthil of preliminary results related to work reported in Ref. 4. He estimates 10 to 20% uncertainty in branching ratios.^h Manthuruthil (see footnote d) reports a level at 2355 ± 2 keV with $\Gamma_0/\Gamma = 0.63$ which may be the same as the level at 2351.

TABLE II. $M1$ strengths and mixing ratios in ^{46}Sc .

Level energy (keV)	$B(E2)^\dagger$ ($e^2 \text{fm}^4$)	$g\Gamma_0(E2)^a$ (meV)	$g\Gamma_0(M1+E2)$ This work (meV)	δ^2 Deduced	$g\Gamma_0(M1)$ Deduced (meV)	$\Gamma_0(M1)/\Gamma_W(M1)^b$
720	72(10) ^c	0.0113(16)	1.58(16)	0.0072(13)	1.57(16)	0.27
1237	154(21) ^c	0.36(5)	0.38(2)	>4.0	<0.08	...
1663	69(21) ^d	0.71(21)	3.87(41)	0.22(7)	3.16(45)	0.033 ^e

^a Derived from column 2.^b Transition strength in W.u.^c Average of values listed in Table 1 of Ref. 3 plus results from Ref. 2 with the results of M. D. Goldberg and B. W. Hooton, Nucl. Phys. **A132**, 369 (1969) omitted from the average.^d R. J. Peterson and D. M. Perlman, Nucl. Phys. **A117**, 185 (1968). Estimated 30% uncertainty not explicitly given by the authors.^e Assuming $g=1.0$.

1. 543-keV Level

The multipolarity of the ground-state transition is known to be $E1$ from internal-conversion coefficient measurements.² The partial width corresponds to 3.8×10^{-4} Weisskopf (W.u.) $E1$ units,

which is normal²⁹ for nuclei in this mass region.

2. 720-keV Level

Our value of Γ_0 is a factor of 2 smaller than the previous resonance-fluorescence result,³⁰ $\Gamma_0 = 5.6$

TABLE III. ^{69}Ga levels and results.

Level energy ^a (keV)	$J\pi$	E_γ This work (keV)	Γ_0/Γ^a	$g\bar{W}\Gamma_0/\Gamma$ This work (meV)	Γ_0 Deduced (meV)
g.s.	$\frac{3}{2}^-$				
318.4(2)	$\frac{1}{2}^-$ ^b	...	1.0	c	...
573.9(2)	$\frac{5}{2}^-$ ^d	574(1)	0.998(2)	0.053(6)	0.035(4)
871.7(2)	$\frac{3}{2}^-$ ^e	872(1)	0.948(5)	1.43(15)	1.51(15)
1027 ^b	$(\frac{1}{2})^-$ ^f	...	0.20 ^b	<0.06	<0.5
1106.4(2)	$\frac{3}{2}^-$ ^g	1106(1)	0.964(2)	2.7(2)	2.8(2)
1336.2(2)	$\frac{7}{2}^-$ ^b	1337(1)	0.937(6)	0.70(4)	1.50(8)
1487.8(2)	$(\frac{1}{2})^+, (\frac{5}{2})^-$ ^f	1488(1)	0.51(5)	0.12(4)	0.23(8) g^{-1}
1525.7(2)	$(\frac{3}{2}, \frac{5}{2})^-$ ^g	...	0.33(3)	<0.06	...
1723.5(4) ^h	$(\frac{5}{2})^-$ ^{g, f}	1723(2)	0.54(8)	0.32(10)	0.40(14)
1890.8(2)	$(\frac{3}{2}, \frac{5}{2})^-$ ^g	1892(2)	0.68(5)	10.3(6)	15.2(15) g^{-1}
1923.0(2)	0.093(9)	<0.4	...
2022.2(2)	$(\frac{3}{2} - \frac{1}{2})^-$ ^g	2024(2)	0.86(5)	2.9(2)	3.4(3) g^{-1}
2042.6(4)	$<\frac{5}{2}$ ^g	2045(2)	0.67(20)	2.1(2)	3.2(10) g^{-1}

^a Reference 8 unless otherwise marked.^b Reference 7.^c No data taken for this level. (See Sec. II in text).^d References 7 and 8. M. M. Khodzaev (Ref. 11) measured A_2 and A_4 coefficients in $(\gamma, \gamma'\theta)$ experiments and deduced $\frac{3}{2}^-$ for this level. A reanalysis of his data indicates that the coefficients are also consistent with a $\frac{5}{2}^-$ assignment.^e Reference 10.^f Reference 9.^g Reference 8.^h This level was studied with electron energy $E_T < 2.04$ MeV to avoid population of the 2043-keV level with its 1724-keV decay to first excited state.

TABLE IV. ^{71}Ga levels and results.

Level energy (keV)	$J\pi^a$	E_γ This work (keV)	Γ_i/Γ^a	$g\bar{W}\Gamma_0\Gamma_0/\Gamma$ This work (meV)	Γ_0 Deduced (meV)
g.s.	$\frac{3}{2}^-$				
389.87(5)	$\frac{1}{2}^-$...	1.0	<0.08	...
487.34(5)	$\frac{5}{2}^-$...	1.0	<0.03	...
511.55(5)	$\frac{3}{2}^-$...	0.91(6)	<0.08 ^b	...
910.3(1)	$\frac{3}{2}^-, (\frac{1}{2}^-)$	910(1)	1.0	0.57(5)	0.57(5) g^{-1}
964.7(1)	$\frac{5}{2}^-$	965(1)	0.78(3)	0.28(5)	0.24(4)
1107.4(2)	$\frac{7}{2}^-$...	0.022(3)
1109.3(5)	$(\frac{1}{2}^-)$	1109(1)	1.0	2.4(3)	4.8(6)
1395.2(4)	$(\frac{5}{2}^-, \frac{7}{2}^-)$	1395(1)	1.0	0.27(6)	0.27(6) g^{-1}
1476.1(2)	$\frac{5}{2}^-, \frac{7}{2}^-$...	0.24(2)	<0.08	...
1493.8(4)	$\frac{9}{2}^+$...	(0.0)	<0.08	...
1498.7(2)	$\frac{5}{2}^-, \frac{7}{2}^-$...	0.0	<0.08	...
1631.6(2)	$\frac{3}{2}^-, (\frac{1}{2}^-)$...	0.093(8)	<0.3	...
1702.1(8)	0.0	<0.3	...
1719.7(7)	$(\frac{5}{2}^-, \frac{7}{2}^-)$	1719(1)	0.43(10)	0.70(18)	1.6(6) g^{-1}
2064.6(2)	$\frac{1}{2}^-, \frac{3}{2}^-$	2064(1)	0.64(9)	1.8(2)	2.9(4) g^{-1}

^a From Ref. 12.

^b A small correction was made for the background 511-keV annihilation γ ray from environmental radiation.

± 1.2 meV. A possible doublet has been suggested in this energy region, with levels at 720 and 725 keV. In the present work there was no indication of a peak at 725 keV with an upper limit of $g\bar{W}(125^{\circ})\Gamma_0\Gamma_0/\Gamma \leq 0.043$ meV.

3. 974-keV Level

Blasi *et al.*² deduced $J^\pi = \frac{7}{2}^+$ for this level, requiring a fast²⁹ $E1$ ground-state transition corresponding to 8.7×10^{-3} W.u.

4. 1237-keV Level

Coulomb excitation and angular-correlation measurements^{3,6} have restricted the possible J^π assignments for this level to $\frac{5}{2}^-, \frac{7}{2}^-$, or $\frac{11}{2}^-$. Zuk *et al.*⁶ found no β decay to the 1237 level, contradicting earlier reports^{2,31,32} which restricted the spin assignment. A recent $(n, n'\gamma)$ result⁵ indicates spin $\frac{11}{2}^-$. We find $g\Gamma_0 \approx g\Gamma_0(E2)$ which lends support to the $\frac{11}{2}^-$ assignment.

TABLE V. Comparison of $^{69,71}\text{Ga}$ widths $g\Gamma_0$ from resonance-fluorescence studies.

Levels (keV)	Langhoff and Frevert (Ref. 14)	$g\Gamma_0$ (meV) Wilson and Booth (Ref. 33)	This work
872	2.0(4)	0.95(40)	1.51(16)
1106	3.8(4)	...	2.8(3)
1106 + 1109	...	7.1(14)	7.2(3)

5. 2341-keV Level

Reference 1 indicated $\frac{1}{2}^-$ or $\frac{3}{2}^-$ as possible spins. Only $E1$, $M1$, and $E2$ transitions have sufficient strength to be observed in resonance fluorescence, so the spin of this level is deduced to be $\frac{3}{2}^-$.

C. ^{69}Ga and ^{71}Ga Results

The transition strengths for ^{69}Ga and ^{71}Ga are presented in Tables III and IV. The γ rays observed in this work are assigned to the isotopes ^{69}Ga and ^{71}Ga on the basis of the energies and the decay schemes of Zoller, Gordon, and Walters.^{8,12} Three new γ rays unambiguously originated from the Ga scatterer. The γ -ray energies are 1971.8 ± 2.0 , 2007.7 ± 2.0 , and 2105.9 ± 2.0 keV with widths of 1.1 ± 0.2 , 1.1 ± 0.1 , 3.0 ± 0.2 meV, respectively, assuming them to be ground-state transitions in ^{69}Ga . These width values must be multiplied by 1.6 for assignment to ^{71}Ga .

1. ^{69}Ga 1106.4- and ^{71}Ga 1109.3-keV Levels

These transitions appeared in spectra as a closely spaced doublet, as shown in Fig. 4. The identification of the doublet is possible from the SAMPO fits, with an energy difference of 2.3 ± 0.5 keV determined here as compared with 2.9 ± 0.5 keV reported by Zoller, Gordon, and Walters. The upper γ ray of our doublet is identified with the transition from the 1109.3-keV level in ^{71}Ga and not with the 1107.4-keV level⁸ γ ray of ^{69}Ga on the ba-

sis of the energy separation and the small (0.022) ground-state branching⁸ of the 1107.4-keV level.

The 1106-1109 doublet was studied by Wilson and Booth³³ in resonant scattering of bremsstrahlung, but only the 1106.4 level in ^{69}Ga was excited by Langhoff and Frevert¹⁴ in resonance fluorescence using a radioactive source. The apparent discrepancy between the results of Wilson and Booth and those of Langhoff and Frevert for the 1106.4-keV level is here resolved. See Table V.

D. Comparison of ^{69}Ga Results with Theory

Listed in columns 7 and 8 of Table VI are the $M1$ and $E2$ transition rates calculated by Paradellis and Hontzeas³⁴ for the first six levels of ^{69}Ga . The experimental total rates, derived from the partial widths Γ_0 in Table III and the branching ratios of Zoller, Gordon, and Walters,⁸ are shown in column 6.

One of the predictions of the model is that some of the excited states are highly collective with strong $E2$ transitions. An example is the $\frac{7}{2}^-$ state, formed by coupling a $p_{3/2}$ to the 2^+ core state. The 1336-keV level in ^{69}Ga may be the $\frac{7}{2}^-$ state, although the calculated transitions rate is about 3 times the experimental value. The most important parameter of the model used in deducing the $E2$ transition rates is the core parameter C . The value of C was obtained from experimental $B(E2)$ values in ^{68}Zn and ^{70}Ge . If the source of the difference between the calculated and experimental $E2$ transition rates is this parameter, one would ex-

TABLE VI. Comparison of ^{69}Ga transition rates with the calculations of Paradellis and Hontzeas.

Initial level (keV)	$J\pi_R$	Final level (keV)	$J\pi_f$	E_γ (keV)	Total rate Exp (10^9 sec^{-1})	Calculated rate ^a (10^9 sec^{-1})	
						$M1$	$E2$
573.9	$\frac{5}{2}^-$	0	$\frac{3}{2}^-$	573.9	54	0.32	1.1
		318.4	$\frac{1}{2}^-$	255.4	<0.2	...	0.08
871.7	$\frac{3}{2}^-$	0	$\frac{3}{2}^-$	871.7	2420	200	162
		318.4	$\frac{1}{2}^-$	553.1	128	230	0.1
1027.0	$\frac{1}{2}^-$	0	$\frac{3}{2}^-$	1027.0	<800	600	240
1106.4	$\frac{3}{2}^-$	0	$\frac{3}{2}^-$	1106.4	4000	1100	0.24
		318.4	$\frac{1}{2}^-$	787.7	47	65	72
		573.9	$\frac{5}{2}^-$	532.4	33	6.0	0.1
		871.7	$\frac{3}{2}^-$	234.4	68	49	0.04
1336.1	$\frac{7}{2}^-$	0	$\frac{3}{2}^-$	1336.1	500	...	1400

^a Reference 19.

pect all calculated $E2$ transition rates to be about 3 times larger than the experimental values. The 1336-keV transition was the only pure $E2$ transition measured by resonance fluorescence except for the limits set on the $\frac{5}{2}^-$ to $\frac{1}{2}^-$ transition (Table VI).

The $M1$ transition rates are a more difficult problem. They are very sensitive to the wave-function structure and depend upon the values of the gyromagnetic ratios g_I , g_R , and g_s for the extra proton. In the Paradellis and Hontzeas calculation the values for these parameters were chosen to reproduce the ground-state moment only. The calculated $M1$ transition rate for the 872-keV transitions, for example, is about an order of magnitude smaller than the experimental number. Paradellis suggests in a private communication³⁴ that this is probably because the wave function for the 872-keV state is unsatisfactory. He points out that the spectroscopic factor for the level in Table II of Ref. 19 is much smaller than the experimental value, suggesting that the chosen constants of the model give incorrect configuration mixing.

ACKNOWLEDGMENTS

We would like to thank Kenneth Wright and the staff of the High Voltage Research Laboratory at Massachusetts Institute of Technology for their generosity and cooperation in this work. We also express our appreciation to John Alman and Tim Grieser and the staff of the Boston University computer center for the fine service they provided with the RAX system. Additional thanks are extended to Ms. Kathy Kent and Ms. Gloria Stone for typing the bulk of this manuscript.

APPENDIX I

The yield of resonantly scattered photons per Coulomb from a transition at energy E_R in nuclei in scatterer S can be written

$$Y(E_R) = \frac{1}{4} N(E_R) \eta \lambda^2 g \bar{W}(125^\circ) \Gamma_0 \Gamma_i / \Gamma = N_c / [C P_f \xi(E_\gamma) G], \quad (1)$$

where

$$G = \frac{1}{N} \sum_{\nu=1}^N \left\{ \left(\frac{R_0 r_0}{R_\nu r_\nu} \right)^2 \exp[-\mu_{pb}(E_\gamma) t_\nu] \times \exp \left[- \sum_{\rho=1}^S \mu_\rho(E_R) X_{\rho\nu}^{\text{IN}} \right] \times \exp \left[- \sum_{\rho=1}^S \mu_\rho(E_\gamma) X_{\rho\nu}^{\text{OUT}} \right] R_{\text{att}} \right\}. \quad (2)$$

N_c is the number of counts in the peak, C is the integrated electron current, $\xi(E_\gamma)$ is the photo-peak efficiency of the detector at the energy of the scattered γ ray E_γ , P_f is the pileup fraction, η is the number of resonant nuclei in the scatterer, and $N(E_R)$ is the incident flux. The flux does not vary by more than 10% over the range of emission angles.³⁵ λ is the wavelength of the scattered photons and $g = (2J_R + 1)/(2J_0 + 1)$. Γ_0 is the radiative width to the ground state, and Γ_i/Γ is the branching ratio to level i . The factor G is the correction due to geometrical effects and absorption of incident and scattered photons in the scatterers and the lead filter, averaged over the volume of scatterer S . The angular distribution of the scattered radiation, averaged over the angles subtended by the scatterer centered about $\theta = 125^\circ$ is $\bar{W}(125^\circ)$. The scatterer is divided into N elemental volumes indexed by ν . R_ν and r_ν are the distances to the ν th volume element from the Pt foil and the detector, respectively. The distances to the center point of the scatterer are R_0 and r_0 . The absorption path length in the lead filter is t_ν . The path lengths in g/cm^2 for electronic absorption in the scatterers, indexed by ρ , are $X_{\rho\nu}^{\text{IN}}$ and $X_{\rho\nu}^{\text{OUT}}$. The energy-dependent electronic-absorption coefficients³⁶ for each scatterer are $\mu_\rho(E)$. R_{att} is the resonance-attenuation factor in which $X_{S\nu}^{\text{OUT}}$ is the path length for resonance absorption of an incident photon. If the Doppler form of the resonant cross section³⁷ is used, the resonant attenuation is

$$R_{\text{att}} = \sum_{m=0}^{\infty} \frac{(-k X_{S\nu}^{\text{IN}})^m}{(m+1)m!}, \quad (3)$$

where $k = \frac{1}{4} n g \lambda^2 \Gamma_0 / (\pi^{1/2} \Delta)$, Δ is the Doppler width,

TABLE VII. Average values of previously reported level widths used for calibration.

Nucleus	Level (keV)	Γ_0 (meV)	Nucleus	Level (keV)	Γ_0 (meV)
⁶³ Cu	670.5	2.07(27)	⁸⁹ Y	1507.4	22(3)
⁶⁵ Cu	768.8	4.83(52)	²⁵ Mg	1613.7	32(5)
⁶³ Cu	961.8	0.623(72)	²⁸ Si	1778.7	0.937(46)
⁶⁴ Zn	991.7	0.224(24)	¹¹ B	2124.4	114(8)
⁶⁸ Zn	1039.2	0.248(52)	²⁷ Al	2210.5	17.3(7)
⁶⁸ Zn	1077.6	0.293(26)	³² S	2230	2.35(27)
⁶⁵ Cu	1115.4	1.54(13)	³¹ P	2233.8	1.69(11)
⁵⁹ Co	1190.5	8.4(5)	²⁷ Al	2979.4	117.4(72)
⁶⁰ Ni	1332.5	0.635(27)	²³ Na	2981.1	94(15)
⁵⁸ Ni	1453.9	0.749(30)	³¹ P	3134.7	63(5)

and n is the number of resonant nuclei per gram. The use of the Doppler form was justified by the subsequent analysis which showed that the smallest Δ/Γ was about 50. The yield formula, Eq. (1), was embodied in a computer program, and the number N of elemental volumes used for computing G was increased until the correction converged near $N = 1000$.

Since we measured only ratios of yields, the absolute detector efficiency is not required. The relative efficiency as a function of energy was established using the known³⁸ relative intensities from a ⁵⁶Co source. The relative efficiency was roughly scaled to the absolute value by comparing the counting rate from the Ge(Li) detector with that from a 8×8-cm NaI detector using a ²²Na source.

APPENDIX II

The literature of transition-strength measurements was thoroughly searched for values to be included in the average used in this work for calibration. The values listed in Table VII are weighted averages of selected measurements including at least 2 and as many as 25 previously reported values for each level. Typical criteria for the rejection of a previous measurement were: electron-tron-scattering results obtained without distorted-wave Born-approximations corrections; preliminary results reported only at conferences; and measurements more than 3 standard deviations from the mean. The uncertainty in the literature width is the propagated individual errors or the rms deviation, whichever is larger.

†Work supported in part by the National Science Foundation. This publication contains work submitted for partial fulfillment of the requirements for the Ph.D. dissertation by one of the authors (RGA). See footnote 28 for reference to preliminary results in ⁴⁵Sc.

*Present address: Department of Physics, American University, Washington, D. C.

‡Present address: The Maret School, 3000 Cathedral Avenue, Washington, D. C.

¹M. B. Lewis, Nucl. Data B4(Nos. 3, 4) 237 (1970).

²P. Blasi, T. F. Fazzini, P. R. Maurenzig, and N. Taccetti, Nuovo Cimento 68, 49 (1970).

³D. A. Eastham and W. R. Phillips, Nucl. Phys. A146, 112 (1970).

⁴F. W. Prosser, D. D. Watson, J. C. Manthuruthil, and D. R. Gilson, Bull. Am. Phys. Soc. 15, 1673 (1970).

⁵V. C. Rogers, L. E. Beghian, F. M. Clikeman, and D. C. Hedengren, Bull. Am. Phys. Soc. 16, 59 (1971).

⁶W. M. Zuk, W. F. Davidson, M. R. Najam, and M. A. Awal, Z. Physik 242, 93 (1971).

⁷D. E. Velkley, K. C. Chung, A. Mittler, J. D. Brandenberger, and M. T. McEllistrem, Phys. Rev. 179, 1090 (1969).

⁸W. H. Zoller, G. E. Gordon, and W. B. Walters, Nucl. Phys. A124, 15 (1969).

⁹R. G. Couch, J. A. Biggerstaff, F. G. Perey, and S. Raman, Phys. Rev. C 2, 149 (1970).

¹⁰S. Raman and R. G. Couch, Phys. Rev. C 2, 744 (1970).

¹¹M. M. Khodzhaev, Yadern. Fiz. 1, 893 (1969) [transl.: Soviet J. Nucl. Phys. 10, 516 (1970)].

¹²W. H. Zoller, W. B. Walters, and G. E. Gordon, Nucl. Phys. A142, 177 (1970).

¹³See references cited in Table II.

¹⁴H. Langhoff and L. Frevert, Nucl. Phys. A111, 225 (1968).

¹⁵J. D. McCullem, B. F. Bayman, and L. Zamick, Phys. Rev. 134, B515 (1964).

¹⁶B. Malik and W. Scholz, Phys. Rev. 150, 919 (1966).

¹⁷I. P. Johnstone, Can. J. Phys. 48, 1208 (1970).

¹⁸W. Scholz and F. B. Malik, Phys. Rev. 176, 1355 (1968).

¹⁹T. Paradellis and S. H. Hontzas, Can. J. Phys. 49, 1750 (1971).

²⁰W. J. Alston, H. H. Wilson, and E. C. Booth, Nucl. Phys. A107, 153 (1968).

²¹F. R. Metzger, Phys. Rev. 187, 1700 (1969).

²²V. K. Rasmussen, Nucl. Phys. A169, 166 (1971).

²³C. P. Swann, Nucl. Phys. A172, 569 (1971).

²⁴R. G. Arnold, Ph.D. dissertation, Boston University, 1972 (unpublished), available from University Microfilms, Inc., Ann Arbor, Michigan.

²⁵The excitation function shape is not the profile of the bremsstrahlung flux below E_T . It is the shape of the incident spectrum at E_R as a function of E_T as the electron energy is increased. For further discussion see Ref. 24.

²⁶Average of results listed in the compilation by S. J. Skorka, J. Hertel, and W. T. Retz-Schmidt, Nucl. Data A4, 347 (1966), with the results of E. C. Booth and co-workers omitted from the average.

²⁷J. T. Routti and S. G. Prussin, Nucl. Instr. Methods 72, 125 (1969).

²⁸Preliminary results for ⁴⁵Sc were reported in R. G. Arnold, E. C. Booth, and W. J. Alston, III, Bull. Am. Phys. Soc. 16, 563 (1971).

²⁹D. H. Wilkinson, in *Nuclear Spectroscopy*, edited by F. Ajzenberg-Selove (Academic, New York, 1960), Pt. B, p. 852.

³⁰N. J. A. Rust and W. L. Mouton, private communication quoted in Ref. 1.

³¹F. T. Porter, M. S. Freedman, F. Wagner, Jr., and K. A. Orlandini, Phys. Rev. 146, 774 (1966).

³²D. Gfoler and A. Flamersfeld, Z. Physik 187, 490 (1965).

³³H. H. Wilson and E. C. Booth, Bull. Am. Phys. Soc. 12, 75 (1967).

³⁴We are indebted to T. Paradellis for private communication of additional calculations not reported in Ref. 19.

and for a helpful discussion of the significance of our results in the framework of his model.

³⁵J. S. Brownson, Ph.D. dissertation, Boston University, 1968 (unpublished), available from University Microfilms, Inc., Ann Arbor, Michigan.

³⁶G. W. Grodstein, "X Ray Attenuation Coefficients,"

National Bureau of Standards Circular No. 583 (1957).

³⁷F. R. Metzger, in *Progress in Nuclear Physics*, edited by O. R. Frisch (Pergamon, New York, 1959).

³⁸A. H. Shere and B. D. Pate, Nucl. Phys. **A112**, 85 (1968).

Resonance-Fluorescence Studies. II. ¹²¹Sb and ¹²³Sb†

Edward C. Booth, Raymond G. Arnold,* and William J. Alston, III

Boston University, Boston, Massachusetts 02215

(Received 27 March 1972)

Resonant scattering of bremsstrahlung was used to measure the scattering widths $gW\Gamma_0\Gamma_i/\Gamma$ for 43 transitions in the antimony isotopes ^{121,123}Sb between 0.5 and 2.5 MeV. Absorption measurements determined $g\Gamma_0$ in seven cases. Comparison of the scattering widths with the $B(E2)$ values from Coulomb excitation gave the mixing ratios in five cases. The theoretical level schemes and $B(E2)$ calculations using the unified model up to second order in the collective variable had some success in explaining the experimental results.

I. INTRODUCTION

This paper reports a study of ¹²¹Sb and ¹²³Sb by the method of bremsstrahlung resonance fluorescence. We measured level widths, increased the level-energy accuracy, and improved the spin assignments for levels in the stable antimony isotopes. This work is part of a series of measurements^{1,2} on ¹¹⁵In, ¹²¹Sb, ¹²³Sb, and ¹²⁷I, which is intended to determine electromagnetic-transition probabilities in nuclei near the closed proton shell at $Z=50$. The reader is referred to Paper I³ containing a detailed description of the experiment, data reduction methods, and error analysis. Recent theoretical work includes that of Sen and Sinha,⁴ Vanden Berghe and Heyde,⁵ and Goldstein and De Pinho.⁶

II. EXPERIMENT

The intensity of resonance-scattered bremsstrahlung is proportional to $g\Gamma_0\Gamma_iW(\theta)/\Gamma$, where $g=(2J_R+1)/(2J_0+1)$, Γ_0 and Γ_i are the partial widths for the ground-state and excited-state transitions, respectively, and $W(\theta)$ is the angular-distribution factor. At our scattering angle $\theta=125^\circ$ we have $0.85 < W(125^\circ) < 1.0$ for ¹²¹Sb and ¹²³Sb. Absorption measurements sometimes can be performed to

obtain $g\Gamma_0$. The multipolarities of transitions observed in bremsstrahlung resonance fluorescence are $E2$, $M1$, and occasionally $E1$, with negligible contribution from higher multipoles. The $E2$ part of Γ_0 in the mixed $M1+E2$ transitions frequently is known from Coulomb excitation, $\alpha\alpha'$, or electron-scattering measurements, so the mixing ratio can be obtained from $\Gamma_0(E2)/[\Gamma_0(M1+E2) - \Gamma_0(E2)]$.

Our target was natural antimony weighing 1600 g with an area of 200 cm². The scattered-photon spectrum was detected with a 40-cm³ Ge(Li) diode. The data are similar to that shown in Paper I. Most of the peaks located by the computer program SAMPO (Paper I) were previously observed in the analog display of the data. The antimony scatterer was alternated with calibration scatterers containing nuclei with levels of known width. In some cases the calibration and antimony scatterers were used simultaneously, giving substantially the same results as the previous method. The scattering measurements consisted of 30 runs between 0.6 and 3.0 MeV with a total running time of about 100 h. Excitation functions were obtained for many of the levels, although only one measurement is required in principle, since the bremsstrahlung flux is known.³ Excitation functions were used to discriminate